digested with S_1 nuclease, precipitated with trichloracetic acid, and passed over GF/C filters (Whatman) for scintillation counting, normalized to amount of TNA. For UCP2 mRNA detection, a 360-base pair *Bgl*II-*Sma*I fragment of mouse *UCP2* cDNA (Genbank accession no. U69135) was subcloned into Bluescript; an antisense riboprobe was synthesized using T3 RNA polymerase and [α^{32}P]-UTP. The hybridization and detection protocol was similar to that used for *UCP1*, except hybrids were digested using RNases A and T1 before acid precipitation.

Hormones. Plasma leptin levels were determined by radioimmunoassay (Linco, St Charles, MO)[25]. Serum thyroid hormone levels were determined by radioimmunoassay (Phoenix, Everett, WA) and mouse TSH levels were determined by radioimmunoassay (AniLytics, Gaithersburg, MD) using the mouse TSH preparation of the National Hormone and Pituitary Institute as a standard.

Physiology. Core body temperature was monitored using a model 43 TA telethermometer and model 402 colonic probe (YSI, Yellow Springs, OH). Oxygen consumption was measured using an Oxymax indirect calorimeter (Columbus, OH). Airflow to the chamber was 0.75 l min^{-1}; samples were taken every minute, with room air reference taken every 30 min. Mice were kept in the chamber for 4–5 h without food or water during the middle of the light cycle. Basal oxygen consumption was determined for each mouse by averaging minimum plateau regions (typically 50–100 data points total), which corresponded to periods of inactivity or sleep. For mice housed at 30 °C the Oxymax chamber was also maintained at 30 °C. Food and water values are the average daily intake over a 5-day period. For DOPS rescue, oxygen consumption was measured beginning ~1 h after a single injection; food and water intake were measured over the next 5 days with injections of DOPS every 12 h; temperature was measured at the end of the 5 days, just before placement at 4 °C.

Peripheral blood flow was assessed using a floLAB Server laser Doppler perfusion monitor and a two-fibre right-angle optical probe (Moor, Millwey, UK). Mice were paralysed with an intraperitoneal injection of D-tubocurarine HCl (Sigma, St Louis, MO) at 0.7 μg per g body weight. About 10 min after injection, the tail was positioned over the probe and lightly fixed in place with tape. The probe and tail were held in place by a custom wooden adapter ~2 × 2 × 1 cm. The probe was repositioned if blood flow was too low for analysing vasoconstriction. Flow was monitored until a stable baseline was achieved, then the whole apparatus was moved to the cold room (4 °C) and left there until a new stable baseline was achieved, usually after about 10 min.

EMGs were recorded by placing mice in a restraining tube and inserting two stainless steel safety pins subcutaneously over the left and right back muscles. The electrical signal was passed through a model M-707 Microprobe amplifier (World Precision Instruments, New Haven, CT) and boosted 121 times through two low-pass filters (Frequency Devices, Model 902). The data was filtered at 1 kHz and collected digitally using an INDEC (Sunnyvale, CA) acquisition board, a computer and Fastlab software.

Received 19 December 1996; accepted 26 March 1997.

1. Landsberg, L. & Young, J. B. Catecholamines and the adrenal medulla. in *Williams Textbook of Endrocrinology* 8th edn (eds Wilson, J. D. & Foster, D. W.) 621–705 (W.B. Saunders, Philadelphia, 1992).
2. Goldman, C. K., Marino, L. & Leibowitz, S. F. Postsynaptic α_2-noradrenergic receptors mediate feeding induced by paraventricular nucleus injection of norepinephrine and clonidine. *Eur. J. Pharmacol.* **115,** 11–19 (1985).
3. Nicholls, D. G. & Locke, R. M. Thermogenic mechanisms in brown fat. *Physiol. Rev.* **64,** 1–64 (1984).
4. Klaus, S., Casteilla, L., Bouillard, F. & Ricquier, D. The uncoupling protein UCP: a membraneous mitochondrial ion carrier exclusively expressed in brown adipose tissue. *Int. J. Biochem.* **23,** 791–801 (1991).
5. Rothwell, N. J. & Stock, M. J. A role for brown adipose tissue in diet-induced thermogenesis. *Nature* **281,** 31–35 (1979).
6. Brooks, S. L. *et al.* Increased proton conductance pathway in brown adipose tissue mitochondria of rats exhibiting diet-induced thermogenesis. *Nature* **286,** 274–276 (1980).
7. Glick, Z., Teague, R. J. & Bray, G. A. Brown adipose tissue: thermogenic response increased by a single low protein, high carbohydrate meal. *Science* **213,** 1125–1127 (1981).
8. Jung, R. T., Shetty, P. S., James, W. P. T., Barrand, M. A. & Callingham, B. A. Reduced thermogenesis in obesity. *Nature* **279,** 322–323 (1979).
9. Bray, G. A., York, D. A. & Fisler, J. S. Experimental obesity: a homeostatic failure due to defective nutrient stimulation of the sympathetic nervous system. *Vitam. Horm.* **45,** 1–125 (1989).
10. Lowell, B. B. *et al.* Development of obesity in transgenic mice after genetic ablation of brown adipose tissue. *Nature* **366,** 740–742 (1993).
11. Hamann, A., Flier, J. S. & Lowell, B. B. Decreased brown fat markedly enhances susceptibility to diet-induced obesity, diabetes, and hyperlipidemia. *Endocrinology* **137,** 21–29 (1996).
12. Susulic, V. S. *et al.* Targeted disruption of the β_3-adrenergic receptor gene. *J. Biol. Chem.* **270,** 29483–29492 (1995).
13. Thomas, S. A., Matsumoto, A. M. & Palmiter, R. D. Noradrenaline is essential for mouse fetal development. *Nature* **374,** 643–646 (1995).
14. Silva, J. E. Full expression of uncoupling protein gene requires the concurrence of norepinephrine and triiodothyronine. *Mol. Endocrinol.* **2,** 706–713 (1988).
15. Geloen, A., Collet, A. J., Guay, G. & Bukowiecki, L. J. β-adrenergic stimulation of brown adipocyte proliferation. *Am. J. Physiol.* **254,** C175–C182 (1988).
16. Enerbäck, S. *et al.* Mice lacking mitochondrial uncoupling protein are cold-sensitive but not obese. *Nature* **387,** 90–94 (1997).
17. Larson, P. R. & Ingbar, S. H. The thyroid gland. In *Williams Textbook of Endocrinology* 8th edn 357–488 (eds Wilson, J. D. & Foster, D. W.) (W.B. Saunders, Philadelphia, 1992).
18. Fleury, C. *et al.* Uncoupling protein-2: a novel gene linked to obesity and hyperinsulinemia. *Nature Genet.* **15,** 269–273 (1997).
19. Siviy, S. M., Kritikos, A., Atrens, D. M. & Shepherd, A. Effects of norepinephrine infused in the paraventricular hypothalamus on energy expenditure in the rat. *Brain Res.* **487,** 79–88 (1989).
20. McGregor, I. S., Menendez, J. A., Atrens, D. M. & Lin, H. Q. Prefrontal cortex α_2 adrenoceptors and energy balance. *Brain Res. Bull.* **26,** 683–691 (1991).
21. Zolovick, A. J., Rossi III, J., Davies, R. F. & Panksepp, J. An improved pharmacoogical procedure for depletion of noradrenaline: pharmacoogy and assessment of noradrenaline-associated behaviors. *Eur. J. Pharmacol.* **77,** 265–271 (1982).
22. Himms-Hagen, J. Role of brown adipose tissue thermogenesis in control of thermoregulatory feeding in rats: a new hypothesis that links thermostatic and glucostatic hypotheses for control of food intake. *Proc. Soc. Exp. Biol. Med.* **208,** 159–169 (1995).
23. Erickson, J. C., Clegg, K. E. & Palmiter, R. D. Sensitivity to leptin and susceptibility to seizures of mice lacking neuropeptide Y. *Nature* **381,** 415–418 (1996).
24. Leibowitz, S. F. Brain neuropeptide Y: an integrator of endocrine, metabolic and behavioral processes. *Brain Res. Bull.* **27,** 333–337 (1991).
25. Ahren, B., Mansson, S., Gingerich, R. L. & Havel, P. J. Regulation of plasma leptin in mice: influence of age, high-fat diet, and fasting. *Am. J. Physiol.* (in the press).

Acknowledgements. We thank Sumitomo Pharmaceuticals, Ltd. (Osaka, Japan) for DOPS; Moor Instruments (Millwey, UK) for loaning their floLAB laser Doppler perfusion monitor; S. C. Woods and R. J. Seeley for use of their indirect calorimeter; C. H. Warden for the *UCP2* clone; P. J. Havel for performing the leptin measurements; B. D. Johnson for help with recording EMGs; A. T. Tafari and C. Kinyoun for technical support; and M. W. Schwartz, D. E. Cummings and J. D. Brunzell for suggestions on the manuscript.

Correspondence and requests for materials should be addressed to R.D.P. (e-mail: palmiter@u.washington.edu).

Hox9 genes and vertebrate limb specification

Martin J. Cohn*†, Ketan Patel*†‡, Robb Krumlauf‡, David G. Wilkinson‡, Jonathan D. W. Clarke* & Cheryll Tickle*

* *Department of Anatomy and Developmental Biology, University College London Medical School, Medawar Building, Gower Street, London WC1E 6BT, UK*
‡ *Division of Developmental Neurobiology, National Institute for Medical Research, The Ridgeway, London NW7 1AA, UK*
† *These authors contributed equally to this work.*

Development of paired appendages at appropriate levels along the primary body axis is a hallmark of the body plan of jawed vertebrates. Hox genes are good candidates for encoding position in lateral plate mesoderm along the body axis[1,2] and thus for determining where limbs are formed. Local application of fibroblast growth factors (FGFs) to the anterior prospective flank of a chick embryo induces development of an ectopic wing, and FGF applied to posterior flank induces an ectopic leg[3]. If particular combinations of Hox gene expression determine where wings and legs develop, then formation of additional limbs from flank should involve changes in Hox gene expression that reflect the type of limb induced. Here we show that the same population of flank cells can be induced to form either a wing or a leg, and that induction of these ectopic limbs is accompanied by specific changes in expression of three Hox genes in lateral plate mesoderm. This then reproduces, in the flank, expression patterns found at normal limb levels. Hox gene expression is reprogrammed in lateral plate mesoderm, but is unaffected in paraxial mesoderm. Independent regulation of Hox gene expression in lateral plate mesoderm may have been a key step in the evolution of paired appendages.

In previous experiments, ectopic formation of limbs induced by FGF suggested the presence of two adjacent cell populations in the flank, one with the potential to form a wing and another with the potential to form a leg[3,4]. To determine directly whether cells that form ectopic wings constitute a separate population from cells that form ectopic legs, a bead soaked in FGF-2 was implanted in the flank either opposite somite (s) 21 (anterior flank), which induces mostly

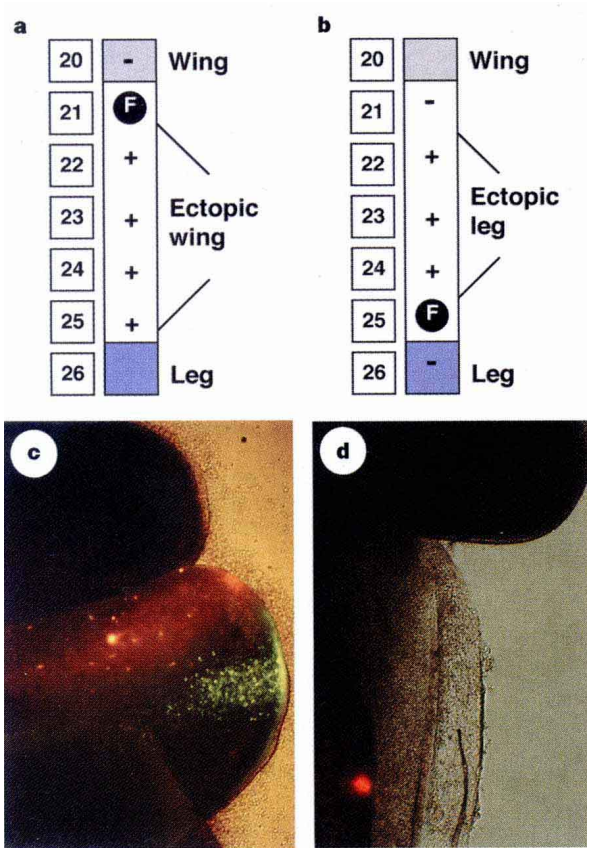

Figure 1 FGF induces bidirectional transformations in flank cell fate to induce ectopic wings and legs. **a**, **b**, Lateral plate mesoderm with FGF bead (F) placed in anterior flank opposite s21 (**a**), a position that generally results in ectopic wing formation, or in posterior flank opposite s25 (**b**), a position that generally results in ectopic legs. FGF beads were implanted in the lateral plate mesoderm of the flank of stage 14–15 chick embryos and a small patch of cells at one or two positions were labelled with DiI and/or DiA at the time of bead implantation. Embryos were viewed under fluorescence microscopy 48 to 72 h later. (+), Cells labelled at this position contributed to the ectopic limb bud; (−), cells labelled at this position did not contribute. (Anterior is at the top.) **a**, When beads were implanted opposite s21, cells labelled opposite s22 ($n = 1$), 23 ($n = 1$), 24 ($n = 3$), and 25 ($n = 1/2$) were located in the ectopic bud. Cells labelled anterior to the bead, opposite s20 in the normal wing, were not detected in ectopic limbs ($n = 2$). **b**, When beads were placed opposite s25, cells labelled opposite s24 ($n = 1$), 23 ($n = 4$), and 22 ($n = 3/4$) contributed to ectopic limbs. Cells in the anterior flank opposite s21 ($n = 3$) and cells posterior to the bead, opposite s26 ($n = 1$), were not detected in ectopic limbs. **c**, Triple exposure photomicrograph of ectopic limb bud to reveal positions of fluorescent cells 72 h after implantation of a FGF bead opposite s25. At the time of bead implantation, flank cells were labelled with DiI (red) opposite s22, and DiA (green) opposite s23. Cells from both positions have contributed to the ectopic limb bud. Note the extent of cell spread in both anteroposterior and proximodistal axes compared to that in a normal embryo (**d**). **d**, Double-exposure photomicrograph of a normal chick embryo in which flank cells opposite s22 had been labelled with DiI 48 h earlier. Labelled cells remain in the flank as a small patch. There is no contribution to the limb buds and cells remained tightly clustered.

Figure 2 Expression of *Hox* group 9 paralogues in lateral plate mesoderm of normal chick embryos and embryos treated with FGF to induce ectopic limbs. *Hoxb9* (**a**, **g**, **k**, **l**, **p** and **q**), *Hoxc9* (**b**, **h**, **m** and **r**) and *Hoxd9* (**c**, **e**, **i**, **n** and **s**) transcripts detected by whole-mount *in situ* hybridization. Embryos are oriented with anterior at the top and are dorsal views, except for **e**, which is a ventrolateral view. Black lines mark boundaries of expression domains in lateral plate mesoderm of normal embryos; arrows mark boundaries on FGF-treated side (except in **i**) and arrowheads are on the contralateral (untreated side) of embryos. **a**–**c**, Pre-limb-bud-stage chick embryos (stage 14–15). **a**, Anterior boundary of *Hoxb9* expression in lateral plate mesoderm lies opposite the junction between s18 and 19. **b**, Anterior boundary of *Hoxc9* in lateral plate mesoderm lies opposite s19. **c**, Anterior boundary of *Hoxd9* in lateral plate mesoderm lies opposite s20–21. These patterns are summarized in **d**, in which the staggering of the boundaries in the prospective wing region is shown. **e**, Stage-16 embryo in which limb budding has been initiated and the anterior boundary of *Hoxd9* has shifted anteriorly from s20–21 to s15 at the anterior margin of the emerging wing bud. **f**, Summary of *Hoxb9*, *c9* and *d9* expression at stage 16. **g**, Stage-18, and **h**, stage-19 chick embryos. The anterior boundaries of *Hoxb9* (**g**) and *Hoxc9* (**h**) are still at the same axial level as in **a** and **b**. In **g**, a clear posterior boundary of *Hoxb9* expression has appeared opposite s26 between the strong flank expression and the weaker leg expression, but no such change is seen in *Hoxc9* (**h**), which is uniformly expressed in flank and leg. **i**, Stage 17–18 embryo. *Hoxd9* is now clearly downregulated in the flank between the wing and leg buds (arrows). **j**, Summary of *Hoxb9*, *Hoxc9* and *Hoxd9* expression at stage 19. Dark and light purple represent intensity of *Hoxb9* expression. **k**, 57 h after application of the FGF bead opposite s23, the posteriorly displaced anterior boundary of *Hoxb9* expression lies at the junction between the ectopic limb bud and the remaining flank (arrow), thereby creating a wing-like pattern in the flank. The boundary of expression on the contralateral side marks the junction between the normal wing bud and anterior flank (arrowhead). **l**, Chick embryo 26 h after implantation of a FGF bead in the lateral plate mesoderm opposite s23. The anterior boundary of *Hoxb9* expression in the lateral plate mesoderm is shifted posteriorly (arrow) compared to the boundary on the contralateral side (arrowhead) which is unaffected. The posterior expression boundary in the lateral plate mesoderm and expression in the somites are unaffected. **m**, **n**, Chick embryos 18 h after application of FGF opposite s21. **m**, The anterior boundary of *Hoxc9* has shifted posteriorly over a distance equivalent to 3 somites (arrow). Compare with contralateral side, where anterior expression boundary lies at the posterior edge of the emerging wing bud (arrowhead). **n**, The anterior boundary of *Hoxd9* remains at the anterior limit of the wing bud, but the domain is posteriorly extended into the flank (arrow), whereas on the contralateral side (arrowhead) *Hoxd9* has been switched off. Note that on the treated (right) side, although the anterior boundary is at the appropriate axial level, the expression in the wing is patchy. By this stage, expression in the leg buds has started to downregulate. **o**, Summary of the patterns of *Hoxb9*, *c9* and *d9* expression in the flank when the flank is anteriorized by FGF to take on a wing identity. **p**, 72 h after application of a FGF bead opposite s24, the posterior boundary of *Hoxb9* expression is no longer visible, as expression in the ectopic bud has taken on a leg-like pattern. *Hoxb9* has been downregulated at the anterior margin of the ectopic bud (asterisk), reproducing the pattern of the normal leg but with a reversed anteroposterior pattern. **q**, 17 h after application of a FGF bead opposite s22, the posterior boundary of *Hoxb9* expression in the lateral plate mesoderm on the treated side has shifted anteriorly (arrow). Expression in the somites and the boundary on the contralateral side (arrowhead) are unaffected. **r**, 19 h after application of FGF opposite s25, the boundaries of *Hoxc9* expression are unaffected. *Hoxc9* is upregulated in the flank around the bead (asterisk and arrow). **s**, 18 h after application of FGF opposite s25, *Hoxd9* expression has been extended throughout the entire flank (arrow). **t**, Summary of the patterns of *Hoxb9*, *c9* and *d9* expression in the flank when the flank is posteriorized by FGF to take on a leg identity.

ectopic wings, or opposite s25 (posterior flank), which induces ectopic legs (wing bud develops opposite s15–20, flank opposite s21–25, and leg bud opposite s26–32) (data from ref. 3; Table 1c). A small number of flank cells were then labelled with the fluorescent dyes DiI or DiA at different distances along the anteroposterior axis from the FGF bead, and the positions of labelled cells were examined 48–72 hours later. FGF beads placed in anterior flank induced an ectopic bud posterior to the bead, and flank cells opposite s22 to 25, the entire span of the prospective flank, were incorporated into the bud ($n = 7$; Fig. 1a). Cells just anterior to the FGF bead did not contribute ($n = 2$). FGF beads placed in posterior flank induced an ectopic limb anterior to the bead, and cells opposite s22 to 24 were seen in ectopic buds ($n = 9$), but neither cells opposite s21 ($n = 3$) nor cells immediately posterior to the bead ($n = 1$) were incorporated (Fig. 1b, c). These results show, rather surprisingly, that when FGF beads are placed at opposite ends of the flank, almost the same population of cells contributes to the ectopic bud, which will form either wing or leg according to the position of the FGF bead. Thus, FGF can induce bidirectional changes in cell fate, and flank cells can be anteriorized to give rise to an ectopic wing or posteriorized to form an ectopic leg.

We next mapped patterns and levels of *Hox* gene expression that characterize different regions of lateral plate mesoderm along the main body axis: prospective wing, prospective leg and the intervening flank. Preliminary observations of *Hoxb9* expression suggested that the anterior boundary of expression in lateral plate mesoderm could be related to limb position, and we therefore focused on expression patterns of *Hox* group 9 paralogues *Hoxb9*,

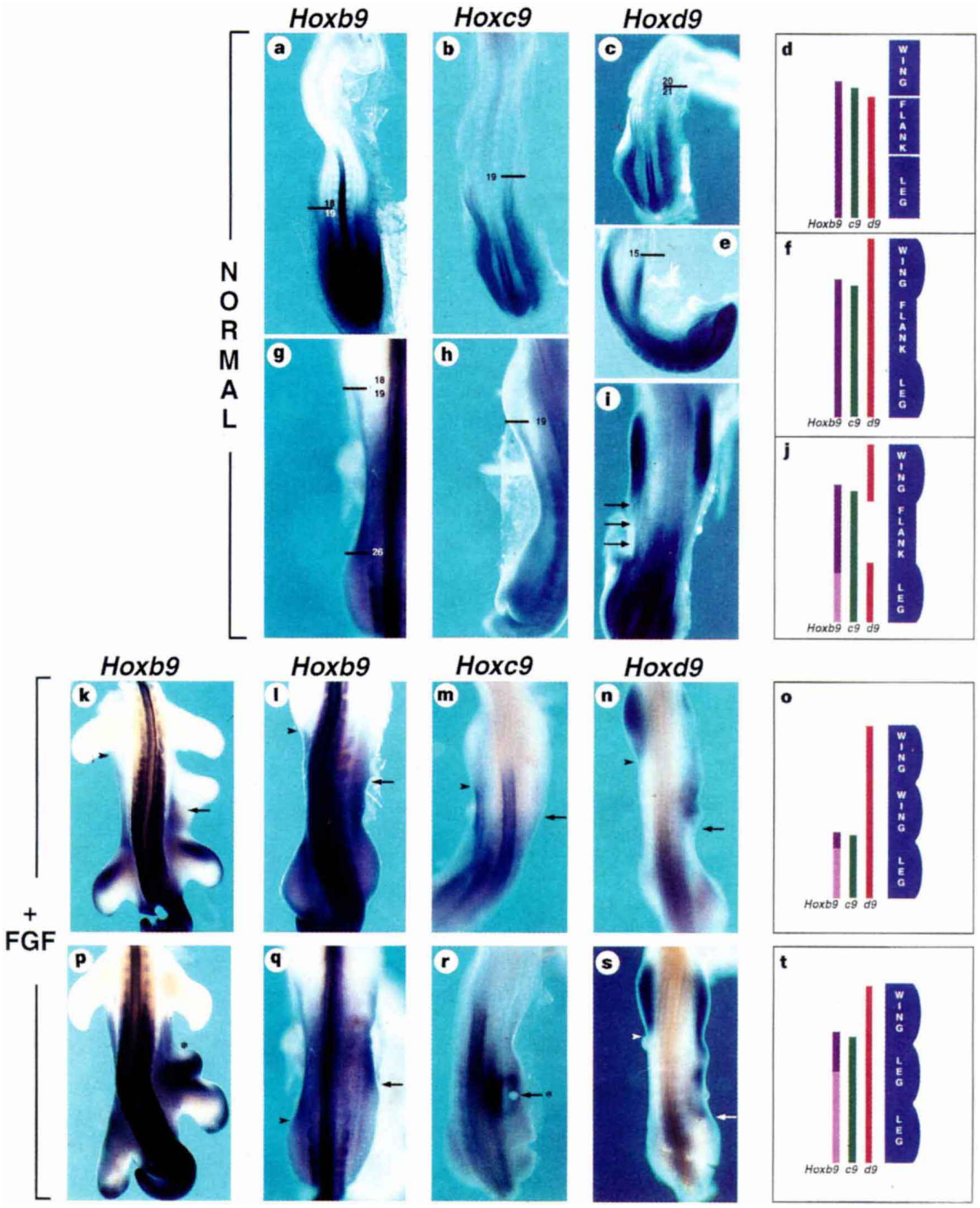

Hoxc9 and *Hoxd9*. Before initiation of limb budding, anterior expression boundaries of *Hoxb9*, *c9* and *d9* in lateral plate mesoderm are staggered within the prospective wing region, and expression is strong throughout prospective flank and leg regions (Fig. 2a–d). This primary pattern of *Hox* gene expression is established very early in development. *Hoxb9* is first expressed around the posterior primitive streak and the domain then spreads anteriorly until the anterior boundary of expression comes to lie within the prospective wing regions at the four-somite stage (data not shown). When limb budding is initiated, a secondary phase of *Hox* gene expression along the main body axis occurs, in which boundaries of expression undergo realignment and levels of expression change locally. The anterior boundary of *Hoxd9* expression shifts anteriorly from the flank–wing junction to the anterior limit of the wing bud (Fig. 2e). Thus, in the secondary phase, the wing bud expresses *Hoxd9* throughout, and *Hoxb9* and *Hoxc9* posteriorly (Fig. 2f). *Hoxd9* expression in the flank is subsequently downregulated and ultimately switches off (Fig. 2i), so that flank expresses *Hoxb9* and *Hoxc9* but not *Hoxd9* (Fig. 2j). *Hoxb9* transcript levels decrease specifically in the leg bud to produce a posterior boundary that separates strong flank expression and weaker leg expression (Fig. 2g), so that the leg bud expression of *Hoxb9* is low and strong for *Hoxc9* and *Hoxd9* (Fig. 2j). Anterior boundaries of *Hoxb9* and *Hoxc9* remain at the same positions as in the primary phase until the buds are well developed (Fig. 2g, h, j; later stages will be described elsewhere). Thus, these three *Hox* genes are expressed in regionally specific patterns related to limb specification and budding.

To determine whether respecification of flank to form limbs involves changes in *Hox* gene expression, we applied FGF to either anterior flank to induce additional wings or to posterior flank to induce additional legs, and monitored expression of *Hoxb9*, *Hoxc9* and *Hoxd9*. We found specific changes in the pattern of *Hox* gene expression in lateral plate mesoderm, according to the position at which FGF is applied. Changes in expression were almost always confined to boundaries; there were no local patches of downregulation around the FGF bead. FGF beads in anterior flank, which lead to ectopic wings, induced a posterior shift of the anterior boundaries of *Hoxb9* and *Hoxc9* expression (Fig. 2k–m; Table 1a,b). The posterior boundary of *Hoxb9* expression could be seen but was not affected (Fig. 2l). In contrast to the posterior shift of *Hoxb9* and *c9* anterior boundaries, the anterior boundary of *Hoxd9* was unaffected, but *Hoxd9* expression was maintained in the flank where it would have been switched off during normal development (Fig. 2n). Thus, the combination of *Hox* genes expressed in the flank after anterior FGF application is transformed from the normal flank pattern to a pattern normally found at wing level (Fig. 2o).

FGF beads in posterior flank, which lead to ectopic legs (Table 1c), induced an anterior shift of the posterior boundary of the *Hoxb9* domain (Fig. 2q; Table 1a), stronger *Hoxc9* expression in the flank (Fig. 2r) and *Hoxd9* expression was again maintained in the flank (Fig. 2s); anterior boundaries of *Hoxb9* and *Hoxc9* were unaffected. These changes transformed the normal flank pattern of *Hox* gene expression to a pattern normally found at leg level (Fig. 2t). FGF applied to mid-flank, opposite s22–24, which results in either wing or leg development, induced shifts of both anterior and posterior boundaries of *Hoxb9*, sometimes in the same embryo (Table 1a, b). FGF beads placed at any position within the flank occasionally induced single lateral outgrowths extending from anterior wing to the posterior limit of the flank ($n = 8$), which were associated with posterior shifts in the *Hoxb9* anterior boundary (Table 1b). Changes in the primary pattern of *Hox* gene expression were detected as early as 12 hours after FGF application, when the anterior boundary of *Hoxb9* had shifted posteriorly in the lateral plate mesoderm over a distance of one somite (Table 1a). Activation of the expression of genes that encode signalling molecules controlling outgrowth and patterning occurs much later in ectopic buds. Ectopic *Fgf-8* transcripts are first detectable in flank ectoderm 14–16 hours after FGF application[5], and ectopic *Shh* is first expressed in flank mesenchyme at 24 hours[3]. Ectopic limb buds later show specific changes in the complex patterns of *Hox* gene expression characteristic of normal wings (for example, downregulation of *Hoxb9*; Fig. 2k) or legs (for example, asymmetric downregulation of *Hoxb9*; Fig. 2p and Table 1b), indicating that a cascade of gene expression characteristic of either wing or leg has been set in train in flank cells.

Hoxb9, *Hoxc9* and *Hoxd9* have different expression boundaries in neural tube, paraxial mesoderm and lateral plate mesoderm. Boundaries of expression in paraxial mesoderm, like lateral plate

Table 1 Effects of FGF on *Hox* gene expression and morphological patterning in lateral plate mesoderm of the flank

(**a**) Pattern of *Hoxb9* expression 12–24 h after application of FGF to the flank

Axial level of FGF bead	Number of embryos assayed	Anterior boundary shifted	Posterior boundary shifted	Both boundaries shifted	Boundaries unchanged
Somite 21	6	3	0	0	3*
Somite 22	3	0	1	0	2
Somite 23	6	3	1	0	2*
Somite 24	1	0	0	1	0
Somite 25	3	0	3	0	0

(**b**) Pattern of *Hoxb9* expression 25–75 h after application of FGF to the flank

Axial level of FGF bead	Number of embryos assayed	Anteriorized wing-like expression pattern	Posteriorized leg-like expression pattern	Expression pattern altered†	Pattern unchanged
Somite 21	9	7 (1‡)	1	0	0
Somite 22	9	3	6	0	0
Somite 23	8	2 (2‡)	1	2	1
Somite 24	9	0 (2‡)	5	1	1
Somite 25	11	2 (3‡)	6	0	0

(**c**) Morphological pattern of ectopic limb skeleton 10 d after FGF application

Axial level of FGF bead	Number of embryos assayed	Ectopic wings	Ectopic legs	Ectopic limbs§	No ectopic limb
Somite 21	8	4	2	0	2
Somite 22	6	4	2	0	0
Somite 23	17	5	4	6	2
Somite 24	12	3	3	2	4
Somite 25	7	0	5	0	2

* Upregulation within expression domain.
† Expression domain altered but without clear resemblance to wing or leg pattern.
‡ Fin-like outgrowth extending from anterior limit of wing to posterior limit of flank.
§ Ectopic limbs with indeterminate morphology.

mesoderm, are dynamic, whereas in neural tube, anterior expression boundaries of *Hoxb9* and *d9* appear to be fixed early and are generally maintained. FGF application to the flank alters *Hoxb9*, *c9* and *d9* boundaries only in lateral plate mesoderm; expression boundaries in somites and neural tube were unchanged (Fig. 2k–n, p–s). This is consistent with our observation that vertebral identity is not altered in embryos that develop ectopic limbs (data not shown).

Our results are consistent with early primary expression of *Hox* genes in lateral plate mesoderm along the body axis specifying positions where limbs develop. Further evidence for this role for *Hox* genes come from mice lacking *Hoxb5*, in which forelimb position is altered[2]. We found that anterior boundaries of *Hox* group 9 paralogues overlap in the region where the wing will form. Staggered boundaries of *Hox* gene expression are known to be important for specifying positional differences along the body axis, as in the distinct segment types in insects[6], the chordate neural tube[7], and the vertebrate axial skeleton[8]. We also found that FGF resets *Hox* expression boundaries in lateral plate mesoderm so that they come to lie in the flank. According to the new pattern of *Hox* gene expression, the same population of flank cells then forms either an additional wing or leg. The fact that an additional limb forms, rather than a shift in position of the nearby normal limb, suggests that limb position has already been specified by a ratchet-like mechanism which irreversibly commits cells. The cascade of gene expression set in train as a result could include the recently identified T-box genes, which are diferentially expressed in forelimbs and hindlimbs and are candidates for specifying limb identity[9]. Although positional identity and *Hox* gene expression is reset in the flank so that an additional limb forms, ectopic limbs have reversed polarity and *Shh* is expressed at the anterior[3,5,10,11]. Thus it appears that polarizing potential in the flank is not reset. Our observation that *Hox* gene expression is altered before activation of *Fgf-8* and *Shh* is reminiscent of the changes in gene expression that enable butterfly prolegs to develop in abdominal segments, when downregulation of *Ubx* and *abd-a* precedes activation of *Antennapedia* (*Antp*) and *Distal-less* (*Dll*) in the prospective limbs[12]. Regulation of *Hox* gene expression patterns is unlikely to be a direct effect of FGF because of the timing. Instead, FGF may interfere with systems that regulate positional identity. Examples of genes known to regulate *Hox* gene expression are *trithorax*- and *Polycomb*-group genes (reviewed in ref. 13). Reduced function of *Mixed-lineage leukaemia* (*Mll*) gene, a mouse homologue of *trithorax*, results in failure to maintain *Hox* genes and leads to simultaneous anteriorization and posteriorization of the vertebral column[14]. If FGF locally interferes with such regulatory genes in lateral plate mesoderm, this could explain how a single factor induces limbs of different types according to where it is applied. The position of paired appendages has shifted along the body axis during evolution without dramatic reorganization of the axial skeleton[15–17], and our finding that *Hox* gene expression can be independently regulated in lateral plate and paraxial mesoderm suggests a mechanism by which this could have occurred. □

Methods

Whole-mount *in situ* hybridization and application of FGF. For whole-mount *in situ* hybridization, embryos were removed from the egg and washed and dissected in 1 × PBS. Embryos were fixed overnight in 4% paraformaldehyde at 4 °C and dehydrated in a series of graded methanol washes. Processing and hybridization were done as described[18], using digoxygenin-labelled riboprobes for the chick genes *Hoxb9*, *Hoxc9* (from C. Tabin) and *Hoxd9* (from D. Duboule). Application of FGF-2 beads was as described[3].

Iontophoretic application of DiI and DiA. Small deposits of the lipophilic membrane dye-DiI (Molecular Probes D-282) and DiA (Molecular Probes D-3883) were applied *in ovo* to the lateral plate mesoderm of the flank and prospective limb bud by iontophoresis. Microelectrodes with a tip diameter of ~3 μm were filled at their tips with a small quantity of DiI or DiA (3 mg ml^{-1} dimethyl formamide) and then backfilled with 1M lithium chloride. These were then inserted into an electrode holder connected to the positive pole of a 9-volt battery. The electrode was carefully micromanipulated through the ectoderm and into the somatic layer of the lateral plate mesoderm at the appropriate position. The dye was driven out of the electrode by completing the circuit with a second silver wire placed into the egg albumin and attached to the battery's negative terminal. Completing the circuit for ~7 s was sufficient to label a small patch of cells. Dye application was done under a dissecting microscope and the success and position of labelled cells then checked on an epifluorescent microscope fitted with an extra long working distance 20 × objective. Embryos were then allowed to develop for the stated times and examined using Nikon fluorescence microscopy. For subsequent analysis of gene expression in labelled embryos, embryos were fixed and mounted in 4% paraformaldehyde, photographed and dehydrated in graded methanol washes before *in situ* hybridization.

Received 19 December 1996; accepted 3 March 1997.

1. Charite, J., de Graaff, W., Shen, S. & Deschamps, J. Ectopic expression of Hoxb-8 causes duplication of the ZPA in the forelimb and homeotic transformation of axial structures. *Cell* **78,** 589–601 (1994).
2. Rancourt, D. E., Tsuzuki, T. & Capecchi, M. R. Genetic interaction between hoxb-5 and hoxb-6 is revealed by nonallelic noncomplementation. *Genes. Dev.* **9,** 108–122 (1995).
3. Cohn, M. J., Izpisùa-Belmonte, J. C., Abud, H., Heath, J. K. & Tickle, C. Fibroblast growth factors induce additional limb development from the flank of chick embryos. *Cell* **80,** 739–746 (1995).
4. Tickle, C. Vertebrate limb development. *Curr. Biol.* **5,** 478–484 (1995).
5. Crossley, P. H., Minowada, G., MacArthur, C. A. & Martin, G. R. Roles for FGF8 in the induction, initiation, and maintenance of chick limb development. *Cell* **84,** 127–136 (1996).
6. Akam, M. *et al.* The evolving role of Hox genes in arthropods. *Development* (suppl.) 209–215 (1994).
7. Lumsden, A. & Krumlauf, R. Patterning the vertebrate neuraxis. *Science* **274,** 1109–1115 (1996).
8. Krumlauf, R. *Hox* genes in vertebrate development. *Cell* **78,** 191–201 (1994).
9. Gibson-Brown, J. J. *et al.* Evidence of a role for T-Box genes in the evolution of limb morphogenesis and specification of forelimb-hindlimb identity. *Mech. Dev.* **56,** 93–101 (1996).
10. Ohuchi, H. *et al.* An additional limb can be induced from the flank of the chick embryo by FGF4. *Biochem. Biophys. Res. Commun.* **209,** 809–816 (1995).
11. Vogel, A., Rodriguez, C. & Izpisùa-Belmonte, J. C. Involvement of FGF-8 in initiation, outgrowth and patterning of the vertebrate limb. *Development* **122,** 1737–1750 (1996).
12. Warren, R. W., Nagy, L., Selegue, J., Gates, J. & Carroll, S. Evolution of homeotic gene regulation and function in flies and butterflies. *Nature* **372,** 458–461 (1994).
13. Simon, J. Locking in stable states of gene expression: transcriptional control during *Drosophila* development. *Curr. Opin. Cell biol.* **7,** 376–385 (1995).
14. Yu, B. D., Hess, J. L., Horning, S. E., Brown, G. A. J. & Korsmeyer, S. J. Altered *Hox* expression and segmental identity in *Mll*-mutant mice. *Nature* **378,** 505–508 (1995).
15. Agar, W. E. The development of the anterior mesoderm, and paired fins with their nerves, in Lepidosiren and Protopterus. *Trans. R. Soc. Edin.* **45,** 611–640 (1907).
16. Goodrich, E. S. *Studies on the Structure and Development of Vertebrates.* (Macmillan, London, 1930).
17. Thorogood, P. & Ferretti, P. Hox genes, fin folds and symmetry. *Nature* **364,** 196 (1993).
18. Nieto, M. A., Patel, K. & Wilkinson, D. G. in *Methods in Avian Embryology* 220–235 (ed. Bronner-Fraser, M.) (Academic, San Diego, 1996).

Acknowledgements. This work was supported by the BBSRC (M.C., C.T.) the MRC (K.P., R.K., D.W.), the Wellcome Trust (K.P., J.C.) and the Astor Foundation (C.T.). We thank M. Coates and R. Nittenberg for stimulating discussions, C. Tabin and D. Duboule for Hox probes, and L. Wolpert for helpful comments on the manuscript.

Correspondence and requests for materials should be addressed to M.C. (m.cohn@ucl.ac.uk).

Essential role for diacylglycerol in protein transport from the yeast Golgi complex

Brian G. Kearns*, Todd P. McGee*, Peter Mayinger†, Alma Gedvilaite*, Scott E. Phillips*, Satoshi Kagiwada* & Vytas A. Bankaitis*

* *Department of Cell Biology, University of Alabama at Birmingham, Birmingham, Alabama 35294-0005, USA*

† *Zentrum für Molekulare Biologie Heidelberg, Im Neuenheimer Feld 282D-69120, Heidelberg, Germany*

Yeast phosphatidylinositol transfer protein (Sec14p) is required for the production of secretory vesicles from the Golgi. This requirement can be relieved by inactivation of the cytosine 5′-diphosphate (CDP)-choline pathway for phosphatidylcholine biosynthesis, indicating that Sec14p is an essential component of a regulatory pathway linking phospholipid metabolism with vesicle trafficking (the Sec14p pathway[1–6]). Sac1p (refs 7 and 8) is